microbial biotechnology

Sustainable biosynthesis of chemicals from methane and glycerol via reconstruction of multi-carbon utilizing pathway in obligate methanotrophic bacteria

Hoa Thi Quynh Le, Anh Duc Nguyen, Ye Rim Park and Eun Yeol Lee[*] iD

Department of Chemical Engineering (Integrated Engineering), Kyung Hee University, 17104, Yongin-si, Gyeonggi-do, South Korea.

Summary

Obligate methanotrophic bacteria can utilize methane, an inexpensive carbon feedstock, as a sole energy and carbon substrate, thus are considered as the only nature-provided biocatalyst for sustainable biomanufacturing of fuels and chemicals from methane. To address the limitation of native C1 metabolism of obligate type I methanotrophs, we proposed a novel platform strain that can utilize methane and multi-carbon substrates, such as glycerol, simultaneously to boost growth rates and chemical production in *Methylotuvimicrobium alcaliphilum 20Z*. To demonstrate the uses of this concept, we reconstructed a 2,3-butanediol biosynthetic pathway and achieved a fourfold higher titer of 2,3-butanediol production by co-utilizing methane and glycerol compared with that of methanotrophic growth. In addition, we reported the creation of a methanotrophic biocatalyst for one-step bioconversion of methane to methanol in which glycerol was used for cell growth, and methane was mainly used for methanol production. After the deletion of genes encoding methanol dehydrogenase (MDH), 11.6 mM methanol was obtained after 72 h using living cells in the absence of any chemical inhibitors of MDH and exogenous NADH source. A further improvement of this bioconversion was attained by using resting cells with a significantly increased titre of 76 mM methanol after 3.5 h with the supply of 40 mM formate. The work presented here provides a novel framework for a variety of approaches in methane-based biomanufacturing.

Introduction

The increasing threat posed by climate change as a result of combustion of fossil fuels has drawn much attention to bio-based production of value-added chemicals and fuels. Methane is among the most potent greenhouse gases, with a short-term global warming potential much greater than that of CO_2 (Clomburg et al., 2017, Hwang et al., 2018). On the contrary, methane is the main component of natural gas and biogas, and its high availability and low cost make it a promising carbon substrate for industrial biotechnology (Haynes and Gonzalez, 2014; Strong et al., 2016). Methanotrophic bacteria can utilize methane as a sole carbon and energy source, giving them the potential to serve as promising hosts for methane sequestration and conversion to diverse biofuels and chemical intermediates (Nguyen et al., 2020a). Despite many attempts to employ methanotrophic bacteria as biocatalysts for methane bioconversion, many technical challenges and limitations to our fundamental knowledge remain to be addressed to this important microbial group (Peyraud et al., 2011, Kalyuzhnaya et al., 2015). Recent efforts to engineer methanotrophs have successfully produced some chemicals and fuels, but only at titres and productivity levels far below those required by industry (Nguyen et al., 2018). Novel engineering strategies are therefore required.

In silico simulation of genome-scale metabolic models in methanotrophs suggests that the reason for the lower yields of target products is not only due to the low efficiency of methane assimilation but also the unbalanced reducing equivalents used in methane oxidation by methane monooxygenase (Akberdin et al., 2018, Bordel et al., 2019). In the other hand, although methane is the most reduced carbon, the supply of electrons from methane to the production of reduced products is limited due to the electron requirements for oxygen splitting during methane oxidation to methanol (Haynes and Gonzalez, 2014). Moreover, the redox-neutral conversion of methane to formaldehyde in methanotrophs results in a 36% energy loss which causes slow growth and low cell yield of methanotrophs on methane (Haynes and Gonzalez, 2014). In addition, the oxidative phosphorylation under aerobic conditions competes reducing power pool in the form of NADH against reduced fuels and

chemicals biosynthesis (Bennett et al., 2018). One possible solution to overcome this issue is to introduce methane utilizing pathway in fast-growing bacteria like *E. coli* in which sugar substrate metabolism might supply reducing power for reduced products. Even though many efforts have been made to heterologously express methane monooxygenase, methanol dehydrogenase, formaldehyde dehydrogenase in a non-native host, this approach faces engineering challenges for chemicals production due to the difficulties in operation of a methanotrophic lifestyle involving multiple-enzyme expression levels, gene regulation and autocatalytic cycle constraints (West et al., 1992, Woolston et al., 2018, Kim et al., 2019, Keller et al., 2020). To date, no heterologous host strain can replace methanotrophic bacteria to efficiently utilize methane as a carbon source for cell growth and production. Therefore, it is important to reconstruct co-metabolism of another reduced substrate together with methane in methanotrophs to boost bacterial growth and provide extra reducing power pool to production of reduced fuels and chemicals.

Enabling methanotrophs as a novel 'platform strain' for production of fuels and chemicals in a more reduced state by co-utilizing methane and reduced multi-carbon substrates would not only increase growth rates, but also provide reducing equivalents to enhance the yields of fuels and chemicals in a more reduced state. The reduced multi-carbon substrate should be inexpensive and abundant in order to be economically feasible substrate. In the current context, glycerol, a by-product of biodiesel production, is a suitable candidate. As biodiesel production increases, crude glycerol as 10% of the total production is generated (He et al., 2017). In fact, the global annual production of glycerol is estimated to reach about 4.2 million tons in 2020, and while the demand for glycerol is predicted to be less than 3.5 million tons (Li et al., 2018, Nomanbhay et al., 2018), this makes crude glycerol simply industrial waste which not only reduces market price but also causes environmental issue. In addition to its high abundance and low cost, high reduced level of glycerol compared with other sugars can deliver more reducing equivalents for a metabolic system (Durnin et al., 2009, Zhang et al., 2013). Moreover, crude glycerol contains a significant level of methanol (Yang et al., 2012, He et al., 2017), which can also be utilized by methanotrophs. It would be advantageous if methanotrophs could utilize crude glycerol without extra purification cost. Thus, the development of methanotrophic platform strain capable of utilizing methane and glycerol can address issue on the limitation of reducing power for the production of target products in a more reduced state and provide solutions to valorize waste materials such as waste methane gas and crude glycerol into value-added products.

To demonstrate the potential of this conceptual design for methanotrophic platform strain, two distinct categories are illustrated in this study. For the first category, we demonstrated that efficient utilization of glycerol as the co-substrate could provide extra reducing power for enhancing reduced product formation. To meet this objective, we reconstructed a mixed heterotrophic mode in *Methylotuvimicrobium alcaliphilum* 20Z for co-metabolism of methane and glycerol to enhance the growth rate and productivity of 2,3-butanediol as a model compound that requires additional NADH in the biosynthetic pathway. For the second category, co-substrate, glycerol, plays a growth-supporting role that results in the novel framework for the bioconversion of methane to methanol. In this approach, we took advantages of methane monooxygenase machinery for alkane oxidation reaction, not whole C1 assimilation metabolism. In this platform strain, glycerol was utilized to sustain cell growth, while methane was directly converted to methanol with complete removal of methanol dehydrogenase (MDH) to prevent further oxidation. In the conventional approach of methane-to-methanol bioconversion, various chemical inhibitors should be added to inhibit MDH, which also inhibit other key enzymes for bioconversion and increase process cost. In our engineered strain, we completely deleted genes encoding MDH that enabled the methane-to-methanol bioconversion without addition of any chemical inhibitor. This study proposes a promising engineering strategy for development of an efficient methanotrophic biocatalyst for sustainable methane-based biorefinery.

Results and discussion

Establishing the effective glycerol-utilizing strain of M. alcaliphilum *20Z*

Two alternative pathways have been proposed for glycerol utilization in *E. coli*, one involving the GlpK-GlpD route under respiratory conditions (Booth, 2005) and the other comprising the GlpA-DhaK route under fermentative conditions (Gonzalez et al., 2008). Glycerol crosses the cell membrane by passive diffusion or via a glycerol-uptake facilitator such as GlpF (Voegele et al., 1993, Maurel et al., 1994). For the respiratory pathway, glycerol is phosphorylated by glycerol kinase (GlpK) to form glycerol 3-phosphate (G3P), which is then oxidized to dihydroxyacetone phosphate (DHAP), simultaneously generates $FADH_2$ by membrane-bounded FAD^+-dependent G3P dehydrogenase (GlpD) and transfers electron to quinone pool in electron transport chain (Booth, 2005). The GlpA-DhaK route is the preferred respiratory pathway for glycerol utilization in terms of providing excess reducing equivalents. Glycerol is dehydrogenated to dihydroxyacetone, and NAD^+ is reduced to NADH by

NAD$^+$-dependent glycerol dehydrogenase (GlpA). DHA is then phosphorylated by ATP- or PEP-dependent DHA kinases (DhaK) to generate DHAP (Gonzalez et al., 2008).

M. alcaliphilum 20Z is an obligate methanotrophic bacterium that is naturally unable to utilize multi-carbon substrates (Akberdin et al., 2018). The strain also does not possess a pathway for glycerol utilization or a glycerol repressor (GlpR). In fact, the wild-type strain was cultured on 0.1% (v/v) glycerol as a sole carbon source; however, no growth was observed (Fig. S1). To enable a synthetic glycerol-utilizing pathway in *M. alcaliphilum* 20Z, a glycerol transporter (GlpF), together with both GlpK-GlpD and GlpA-DhaK routes, has been separately constructed into a pAWP89 backbone vector under control of a P$_{tac}$ promoter (Fig. 1). In both pathways, catabolic flux of glycerol is expected to be incorporated into central metabolism at the DHAP node and then bifurcated towards the ribulose monophosphate and tricarboxylic acid cycles via the gluconeogenic and glycolytic fluxes as a result of fructose-bisphosphate aldolase (FbaA) and triosephosphate isomerase (Tpi) activity, respectively (Fig. 1). The results showed that *M. alcaliphilum* 20Z strain harbouring a GlpA-DhaK route did not grow on glycerol. This may be due to the fact that the GlpA-DhaK route is functionally active in *E. coli* under anaerobic conditions; thus, the GlpA-DhaK route may be inactive under aerobic conditions associated with cultivation of *M. alcaliphilum* 20Z. Although glycerol can be utilized under both aerobic and anaerobic conditions, the process of co-utilizing glycerol with methane to enhance growth rates and productivity needs to be carried out under aerobic conditions because of methane oxidation, and the fermentative pathway is not suitable for methanotrophs in this context. Unlike the GlpA-DhaK route, growth of the engineered strain (20Z_FKD) with GlpK-GlpD routes was observed in 0.1% (v/v) glycerol, with a relatively low optical cell density (OD$_{600}$) of 0.3
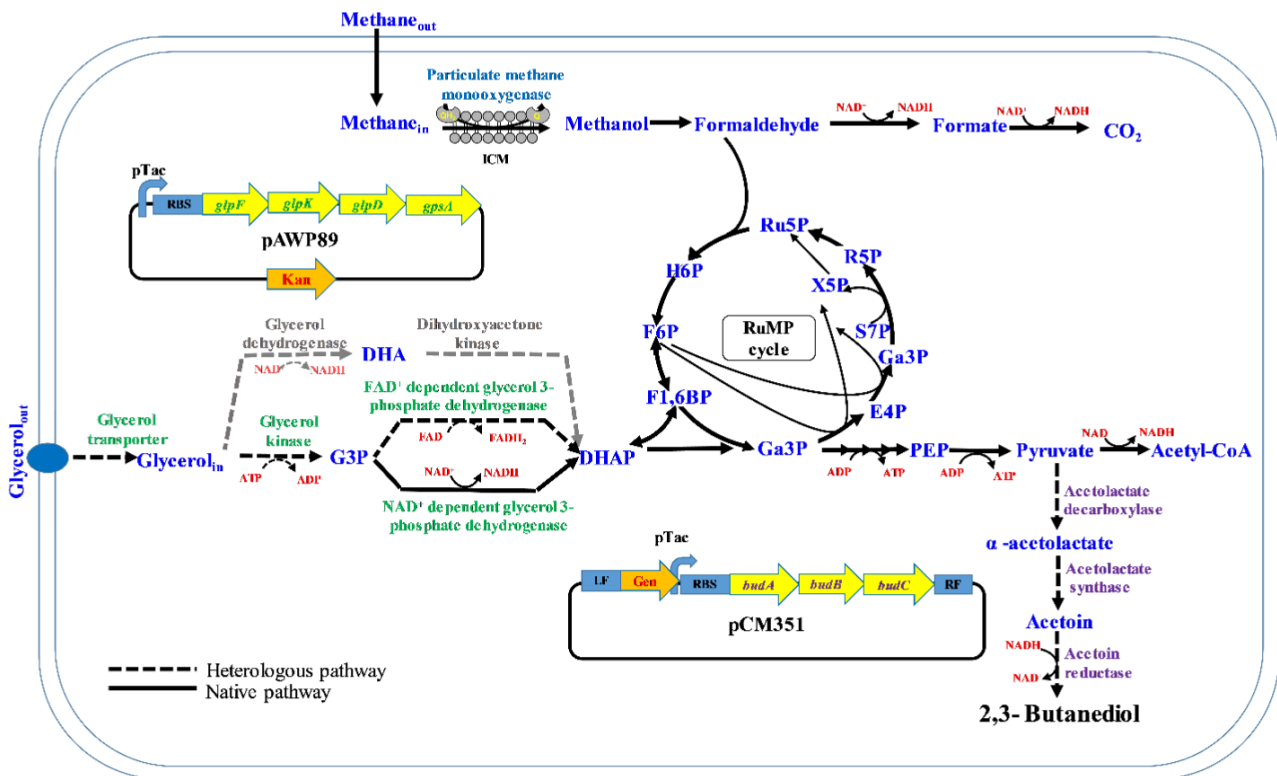

Fig. 1. Metabolic engineering strategy of 2,3-BDO production by co-utilization of methane and glycerol using engineered *M. alcaliphilum* 20Z. Two pathways are proposed for glycerol utilization in methanotrophs, involving the GlpK-GlpD route and the GlpA-DhaK route. Glycerol crosses the cell membrane by passive diffusion or via a glycerol-uptake facilitator (GlpF). In cells, glycerol is incorporated into central metabolism as dihydroxyacetone phosphate (DHAP), a metabolite that can participate in both gluconeogenic and glycolytic processes. Both pathways were constructed in a pAWP89 vector under control of the P$_{tac}$ promoter. For 2,3-BDO production, three-gene cluster *budABC* encoding acetolactate decarboxylase (BudA), acetolactate synthase (BudB) and acetoin reductase (BudC) were integrated into the chromosome of *M. alcaliphilum* 20Z under control of P$_{tac}$ promoter. Ru5P: ribulose 5-phosphate, H6P: hexulose 6-phosphate, F6P: fructose 6-phosphate, KDPG: 2-keto-3-deoxy 6-phosphogluconate, F1,6BP: fructose 1,6-bisphosphate, DHAP: dihydroxyacetone phosphate, G3P: glyceraldehyde 3-phosphate, PEP: phosphoenolpyruvate, OAA: oxaloacetic acid, G3P (convert from glycerol): glycerol 3-phosphate, DHA: dihydroxyacetone. ICM: intracytoplasmic membrane.

after 40 h (Fig. S1). Previously, the poor growth on glycerol of some bacteria was also reported, and it was suggested that this glycerol utilization pathway might be toxic for cells due to unbalanced redox power (Kang et al., 2014), allosteric inhibition (Applebee et al., 2011, Zhan et al., 2018) or intermediate toxicity (Rittmann et al., 2008). In *E. coli*, the *glpFK* operon is tightly controlled by the Glp repressor, which is not present in *M. alcaliphilum* 20Z, and expression of two-gene cluster *glpFK* may not be the main reason for poor growth on glycerol in this engineered strain (Weissenborn et al., 1992). It has been inferred that conversion of G3P to DHAP is a rate-limiting step because of unfunctional expression of a recombinant, membrane-binding enzyme, FAD$^+$-dependent GlpD, in an ultrastructure membrane system of methanotrophs due to saturation of the capacity of the Sec-translocon in native strain (Zhang et al., 2015). It has been reported that accumulation of G3P inhibits cell growth under high activity of glycerol kinase, a cytoplasmic enzyme (Applebee et al., 2011). In addition, DHAP was excluded because this is a branch point in central metabolism of methanotrophs, and cells have mechanisms that convert further DHAP. Therefore, to improve carbon flux for biomass synthesis, generate reducing equivalents, especially NADH, and enhance oxidation of G3P to DHAP, it was necessary to express another alternatively soluble enzyme. We found a version of NAD$^+$-dependent G3P dehydrogenase (GpsA) that is encoded by *gpsA* gene from *M. alcaliphilum* 20Z (MEALZ_0434). This gene was co-overexpressed with three genes *glpFKD*, resulting in the 20Z_FKDA strain, which exhibited a higher growth rate on glycerol than in 20Z_FKD, reaching a final OD$_{600}$ of 1.4 and consuming $\sim$ 1 g l^{-1} glycerol (Fig. 2A). In summary, overexpression of *gpsA* gene along with *glpFKD* enabled sustainable growth of *M. alcaliphilum* 20Z on glycerol. Although enzyme activity of GpsA has not been assayed in *M. alcaliphilum* 20Z, the existence of an orthologous gene in *E. coli*, as shown by experimental evidence at the protein level, indicated that G3P can be converted into DHAP and generate NADH simultaneously (Rho and Choi, 2018).

Given that glycerol as an abundant, cheap substrate, it is significant to screen strains which can grow on the maximum glycerol concentration to enhance cell growth. To define allowing elimination for growth and effective metabolism on glycerol, the 20Z_FKDA strain was cultured on medium containing glycerol concentrations of 0.5% (v/v) and 1% (v/v), but the growth rate was even lower than that on the 0.1% (v/v) glycerol concentration and resulted in dead phase earlier than usual (Fig. 2B). It is inferred that glycerol could significantly influence on the osmotic potential and inhibit growth (Szymanowska-Powałowska, 2015). To overcome this issue and adapt

to increased glycerol concentrations, we deployed adaptive laboratory evolution for the 20Z_FKDA strain. After 50 cycles of sub-culturing for adaptive laboratory evolution, the 20Z_FKDA strain could grow on 1% (v/v) glycerol and achieved a significantly higher growth rate compared with cells grown on 0.1% (v/v) glycerol after 60 h (Fig. 2C and D).

Improvement of 2,3-BDO production by enabling the growth of M. alcaliphilum *20Z on mixed substrate of glycerol and methane*

Because of the limited growth rates and low product yields of methanotrophs on methane compared with other host strains, commercial production of value-added compounds is restricted in methanotrophs. In addition to a systematic approach to improving carbon flux towards target products, co-utilization of alternative, inexpensive substrates represents a feasible strategy to achieve high productivity or yield of desired products. Given its availability, low prices and a high degree of reduction, glycerol is an ideal feedstock to enhance carbon flux in building blocks as well as reducing equivalents for enhancing titre or productivity of value-added chemical production by methanotrophs.

2,3-BDO is a bulk platform chemical with a variety of applications in the chemical, plastic, pharmaceutical, cosmetic and food industries (do Carmo Dias et al., 2018; Yang and Zhang, 2018). Our previous work demonstrated a systematic engineering approach for 2,3-BDO production in a triple-mutant strain of *M. alcaliphilum* 20Z by expressing acetolactate decarboxylase (BudA), acetolactate synthase (BudB), and acetoin reductase (BudC) from *K. pneumoniae* in a plasmid-based expression system which produced 68.8 mg l^{-1} of 2,3-BDO from methane in batch culture (Nguyen et al., 2018). We also found that NADH supply is a key limiting step of 2,3-BDO production in engineered *M. alcaliphilum* 20Z (Nguyen et al., 2018). It is inferred that the unbalanced reducing equivalents used in methane oxidation by methane monooxygenase cause the low productivity of compounds that requires additional NADH in the biosynthetic pathway (Akberdin et al., 2018, Bordel et al., 2019). Utilizing co-substrates that provide extra reducing power would therefore be a feasible strategy to compensate the deficiency of reducing power in the biosynthetic pathway to achieve high productivity or yield of reduced compounds like 2,3-BDO, lactate, ethanol and alanine (Durnin et al., 2009, Li et al., 2018). Theoretically, 20Z_FKDA strain generates excess NADH by activity of NAD$^+$ glycerol-3 phosphate dehydrogenase (GpsA), while the last step of 2,3-BDO biosynthesis requires NADH as a cofactor for conversion of acetoin to 2,3-BDO. The coupling of these reactions can self-
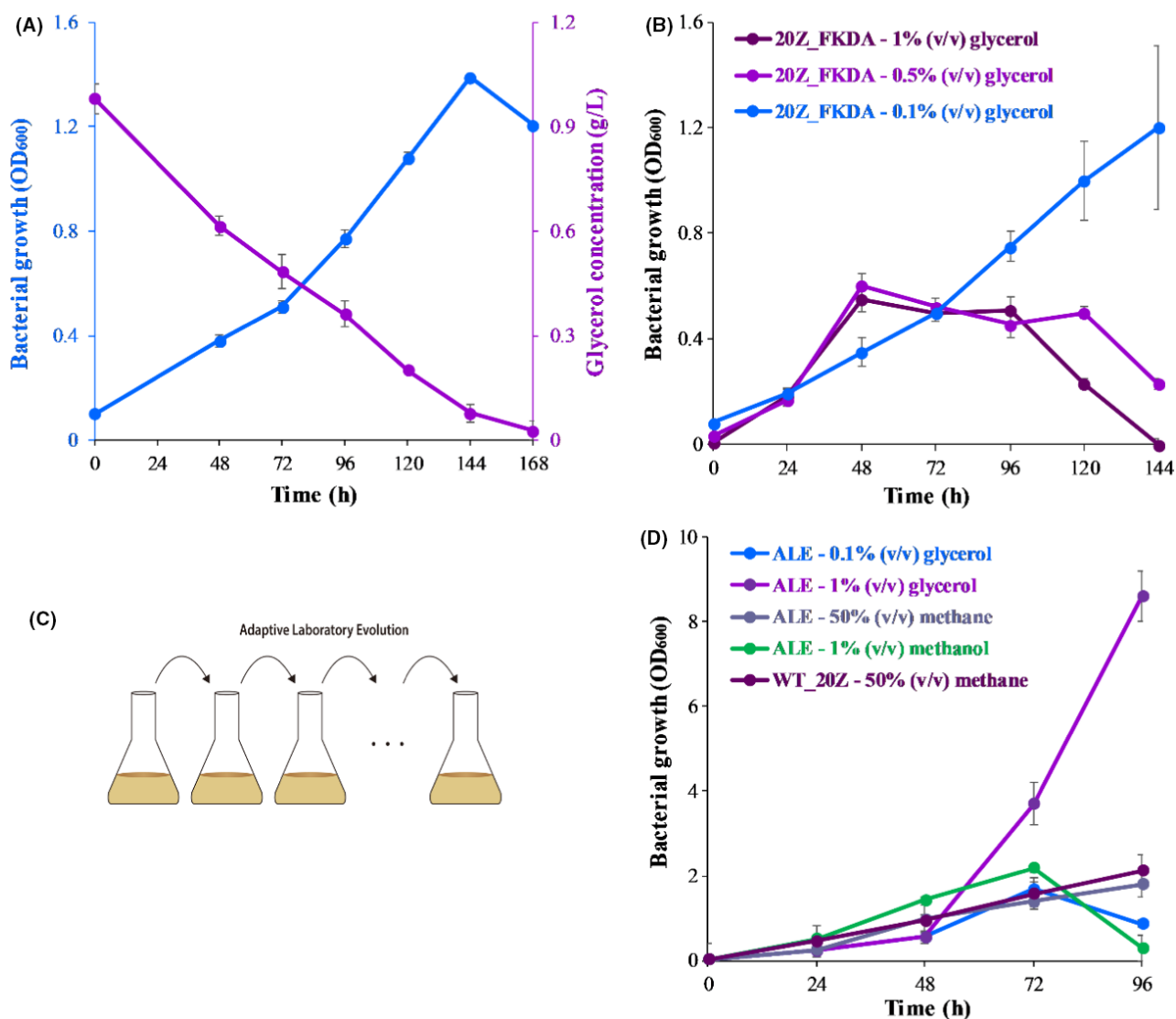
Fig. 2. Glycerol utilization of *M. alcaliphilum* 20Z.
A. Growth rate of glycerol-utilizing strain 20Z_FKDA and glycerol consumption.
B. Effect of glycerol concentrations on growth of the 20Z_FKDA strain.
C and D. Effect of adaptive laboratory evolution on the growth rate of 20Z_FKDA at higher concentration of glycerol. More than 50 repetitions of sub-culturing for adaptive laboratory evolution were carried out with gradually increased glycerol concentration until reaching 1% (v/v) ~ 10 g l^{-1}. Data represent mean and standard derivation (SD) of two independent experimental replicates.

balance intracellular NADH/NAD$^+$ ratio which affects the yield of 2,3-BDO.

To determine whether glycerol does indeed enhance the reducing power pool in cells, 20Z_FKDA strain was separately cultured on 50% (v/v) methane, 0.1% (v/v) glycerol, and co-substrates including 50% (v/v) methane and 0.1% (v/v) glycerol to quantify cellular concentrations of NADH, NAD$^+$ and NADH/NAD$^+$ ratio. To avoid the measurement difference of intracellular concentrations of NADH and NAD$^+$ due to the different cell densities, samples were collected at mid-log phase with the same optical density. The results showed that cytoplasmic NADH concentration on co-substrates utilization was 0.21 mM which was significantly higher than that of sole methane utilization of 0.17 mM (Fig. 3A). Similarly, NADH/NAD$^+$ ratio significantly increased from 0.59 to 0.93 on methane and co-substrates utilization, respectively (Fig. 3B). Moreover, a higher concentration of NAD$^+$ was observed on sole methane utilization (Fig. 3A). Obviously, these results demonstrated that utilization of glycerol could generate extra cytoplasmic NADH and therefore provide more reducing power for 2,3 BDO production.

Although plasmid-based heterologous expression was promising, the metabolic burden and genetic instability of
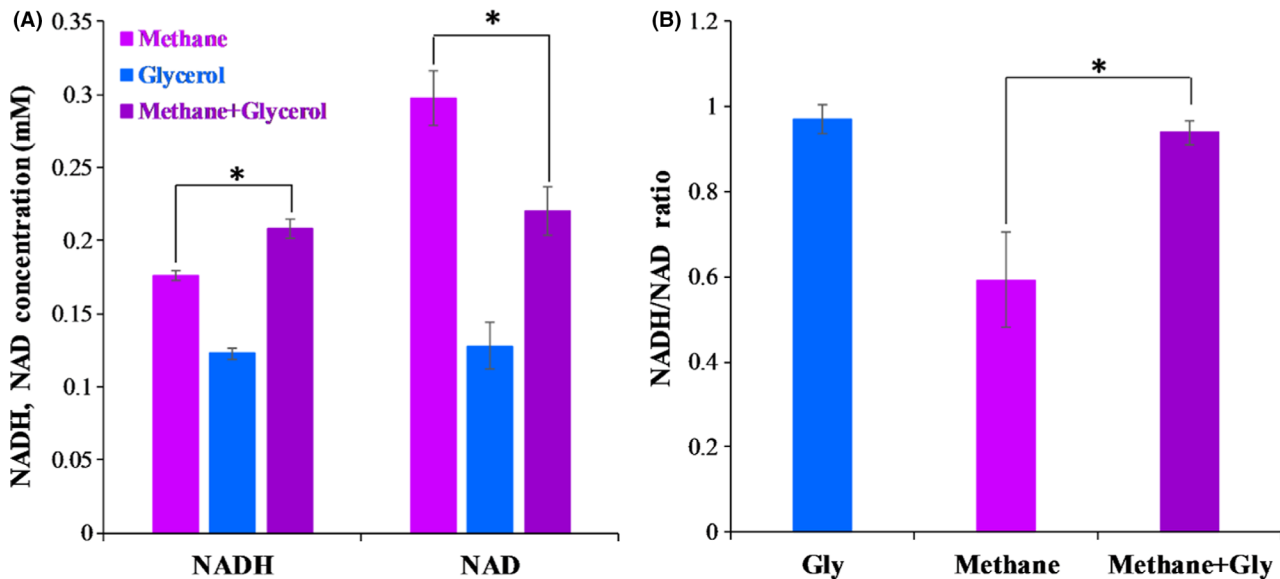
Fig. 3. NADH and NAD$^+$ redox status in cell growth of 20Z_FKDA strain on 50% (v/v) methane, 0.1% (v/v) glycerol, and co-substrates including 50% (v/v) methane and 0.1% (v/v) glycerol at mid-log phase. (A) NADH, NAD$^+$ concentration, (B) NADH/NAD$^+$ ratio. (*$P < 0.05$ methane versus co-substrates groups by Student's *t*-test). Data represent mean and standard derivation (SD) of two independent experimental replicates.

the plasmid precluded industrial applications (Rugbjerg et al., 2018; Rugbjerg and Sommer, 2019). Therefore, chromosomal integration of heterologous metabolic pathways is optimal for industrially relevant fermentation (Rugbjerg et al., 2018; Rugbjerg and Sommer, 2019). Moreover, because 20Z_FKDA already harboured an IncP-based broad-host-range plasmid for expression of *glpF, glpK, glpD,* and *gpsA* genes, we integrated a 2,3-BDO biosynthesis pathway including three-gene cluster *budABC* into the chromosome of *M. alcaliphilum* 20Z to circumvent such problems (Fig. 1). The chromosomal integration was conducted to replace the *glgA1* loci. The 2,3-BDO gene cluster from *K. pneumoniae* under control of the P$_{tac}$ promoter were amplified from pBudK.p and subsequently ligated into a pCM351-*glgA1* vector, generating pCM351-*budABC*. The pCM351-*budABC* vector was transformed into *M. alcaliphilum* 20Z via electroporation, and production of 2,3-BDO was monitored in flask cultures. The resulting strain produced 17.6 mg l^{-1} 2,3-BDO in shake flasks after 144 h using methane as a sole carbon source (Fig. 4B). Likewise, 46 mg l^{-1} 2,3-BDO was accumulated when glycerol was used as a sole carbon source. Interestingly, there was a dramatic increase in growth rate of 20Z_FKDA_*budABC* with mixed substrates, compared to that with a single substrate (Fig. 4A). The doubling time of 20Z_FKDA_*budABC* strain with mixed substrates was 13 h (specific growth rate = 0.052 h^{-1}), which is twofold faster than that of the 20Z_FKDA_*budABC* strain cultured solely on methane, 28 h (specific growth rate = 0.024 h^{-1}) and 1.2-fold faster than that of the 20Z_FKDA_*budABC*

strain cultured solely on glycerol, 16 h (specific growth rate = 0.043 h^{-1}). In agreement with this observation, 68 mg l^{-1} 2,3-BDO was produced when 20Z_FKDA_*budABC* strain cultured on methane plus glycerol after 144 h with 90 mg methane and 2.5 g glycerol were concurrently consumed for co-utilization (Fig. 4C).

It should be noted that the 2,3-BDO production when the 2,3-BDO biosynthesis gene cluster was integrated into the genome was much lower compared to a plasmid-based system (Nguyen et al., 2018), probably due to the lower copy number of the gene of interest on chromosome compared to the case of a multi-copy broad-host-range plasmid (Mustakhimov et al., 2016). Likewise, the transcriptional levels of three genes *budA, budB,* and *budC* via plasmid-based expression might be quantitatively higher than that of genome-integrated expression. To assess this assumption, the transcriptional analysis of *budA, budB* and *budC* was conducted to determine the effect of heterologous protein expression manners. The results showed that the transcriptional level of three genes *budA, budB,* and *budC* via plasmid-based expression was higher than that of genome-integrated expression with statistical significance ($P < 0.05$) (Fig. 5). Therefore, the development of other replicable plasmids in *M. alcaliphilum* 20Z is required to facilitate the metabolic engineering in this particular strain. Moreover, some systematic approaches including RBS optimization as well as gene knockout might be useful for further improvement of 2,3-BDO titre (Nguyen et al., 2018). By using a similar approach, glycerol also was co-utilized with carbon dioxide in an obligate
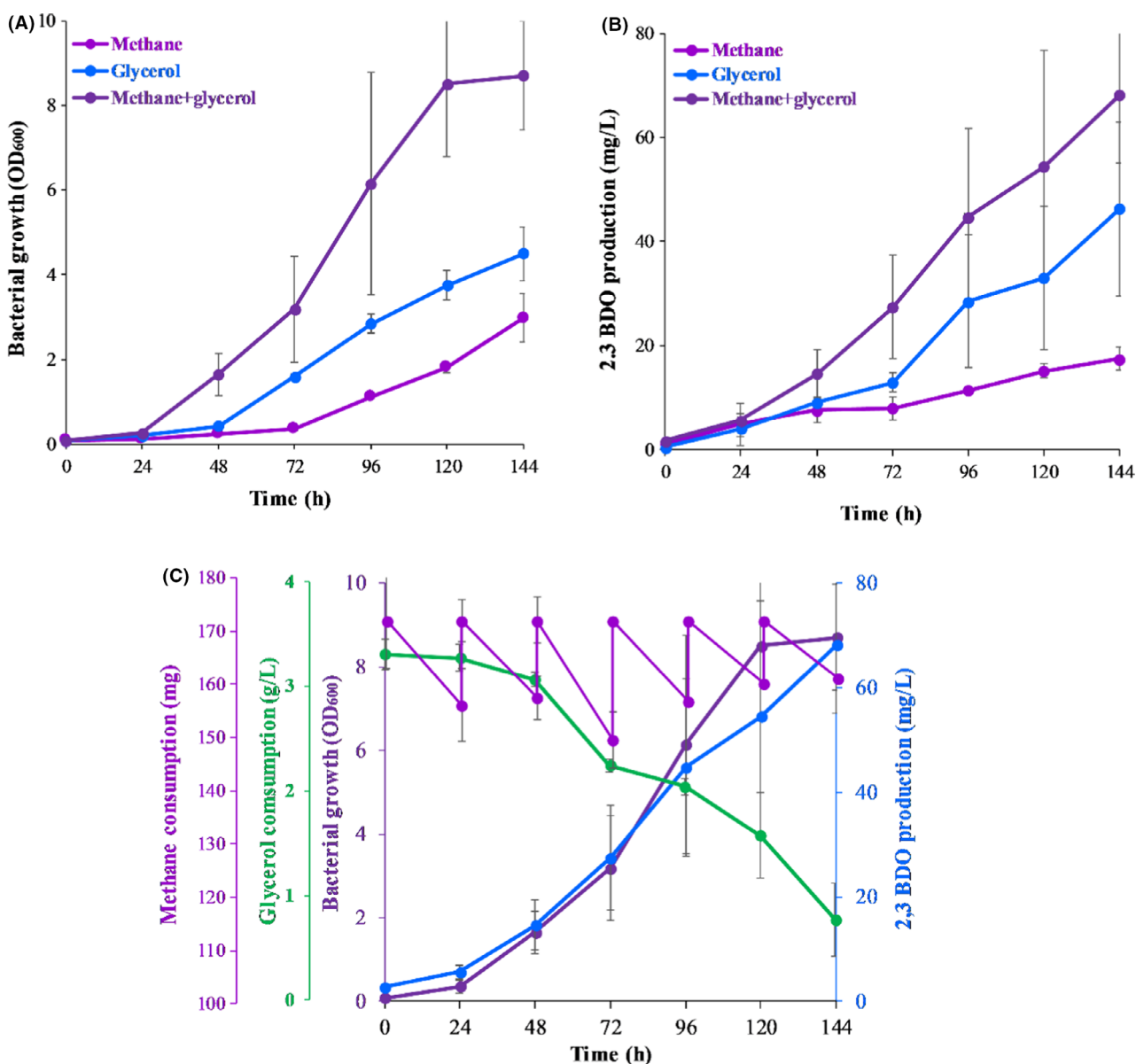
Fig. 4. Effects of co-substrate utilization on growth and 2,3 BDO production of the 20Z_FKDA_*budABC* strain.
A. Growth of engineered strain on sole substrate and co-substrates, (B) 2,3-BDO production on sole substrate and co-substrates.
C. The correlation of methane and glycerol consumption to growth and 2,3 BDO production when culturing on co-substrates. The headspace of the shake flask was refreshed with 50% (v/v) methane every 24 h, and 0.35% (v/v) glycerol (3.5 g l^{-1}) was initially supplied for utilization of sole glycerol and co-substrates. Data represent mean and standard derivation (SD) of two independent experimental replicates.

photoautotrophic cyanobacterium to enhance 2,3-BDO production, the engineered strain of *Synechococcus elongatus* PCC 7942 produced 761 mg 2,3-BDO/L, a 290% increase over the control strain under continuous light conditions (Kanno and Atsumi, 2017). Although our titres and productivity levels of 2,3-BDO are still far below those required by industry, the results demonstrated a proof of concept for utilizing glycerol as a co-substrate to enhance the titre of not only 2,3-BDO, but other industrial chemicals in a methanotroph-based biorefinery.

Development of one-step biocatalyst for direct conversion of methane to methanol

Methane-to-methanol conversion has received research attention due to the demand for sustainable technologies of gas-to-liquid conversion. Recently, the 'methanol economy' has become a promising alternative solution to fossil fuels because it is suitable for use in the current transportation fuel infrastructure, has a greater energy density, and burns with fewer toxic by-products. Due to the high bond energies of the C–H bond in methane
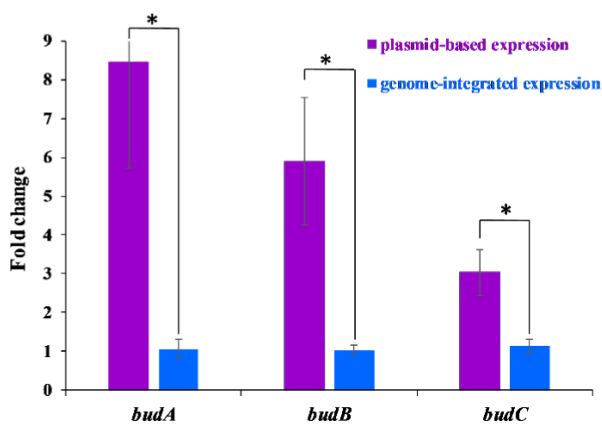
Fig. 5. Comparison of real-time qPCR analysis of *budA*, *budB,* and *budC* gene expression via plasmid-based expression and genomic-integrated expression in *M. alcaliphilum 20Z*. This bar graph represents the fold changes of gene expression quantified by normalization to the RNA polymerase sigma factor *rpoD* (*$P < 0.05$, plasmid-based expression versus genome-integrated expression groups by Student's *t* test). Data represent mean and standard derivation (SD) of three independent experimental replicates.

among organic substrates, the development of efficient catalysts for direct conversion of methane to methanol remains one of the most challenging tasks in catalytic chemistry (Kamachi and Okura, 2018). Enzyme-catalyzed oxidation of methane to methanol has several advantages over thermochemical oxidation reactions, including higher selectivity, improved process efficiency and safer, milder reaction conditions and energy savings, all leading to associated economic benefits (Hwang et al., 2018).

Conversion of methane to methanol using methanotrophs has been considered as an efficient model for methane liquefaction compared with traditional methods (Hwang et al., 2018). To date, whole-cell biocatalysts are a preferred option for bioconversion of methane to methanol due to the relatively low cost of this method. In brief, these bioconversions involve culturing cells on methane during the growth phase and supplying suitable bioconversion inhibitors for MDH. It is clear that accumulation of methanol cannot be achieved by wild-type methanotrophs because methanol is an intermediate metabolite in methane metabolism. To prevent oxidation of methanol, MDH inhibitors are absolutely needed such as phosphate, ethylenediaminetetraacetic acid, cyclopropanol, and high concentrations of NaCl (Hwang et al., 2014, Sirajuddin et al., 2014, Miyaji et al., 2019). Despite being the currently preferred option, whole-cell biocatalysts suffer from several disadvantages, including difficulties at high cell densities, biphasic growth processes for cell growth, and methane conversion by the addition of chemical MDH inhibitors that can also inhibit other key enzymes. On the other hand, whole-cell bioconversions require supplemental exogenous NADH to enhance MMO activity (Haynes and Gonzalez, 2014; Hwang et al., 2014), reducing its cost-effectiveness at commercial scales (Weckbecker et al., 2010, Uppada et al., 2014). An endogenous regeneration system of reduced nicotinamide cofactors is therefore crucial. Theoretically, utilization of co-substrates including glycerol and methane can circumvent this issue. To be more precise, glycerol metabolism in our engineered strain can generate reducing equivalents in terms of NADH and $FADH_2$, which deposit their electrons to quinone pool via complex I of electron transport chain or membrane-bound FAD^+-dependent G3P dehydrogenase and subsequently used to activate particulate methane monooxygenase (pMMO) (Fig. 6).

Our engineered methanotroph strain possessed broader metabolic capacities with the expanded substrate spectrum from C1 (methane) to C3 (glycerol) compounds, which endowed a possibility of removing methanol dehydrogenase that is essential enzyme of C1 metabolism in methanotrophs (Fig. 6). In which, glycerol was utilized to sustain cell growth and provide reducing equivalents for pMMO activity, while methane or ethane was directly converted to methanol or ethanol without further oxidation. In *M. alcaliphilum 20Z*, methanol oxidation is catalyzed by the periplasmic pyrroloquinoline quinone-linked methanol dehydrogenase including calcium-dependent MDH and lanthanum-dependent MDH (Vuilleumier et al., 2012). Genes encoding calcium-dependent MDH, *mxaFI*, and the lanthanum-dependent MDH, *xoxF* from *M. alcaliphilum 20Z* were completely knocked out (Fig. S3), resulting in the 20Z_M2 strain. As we expected, the 20Z_M2 strain no longer grew on C1 substrates (Fig. S2), indicating complete deletion of methanol dehydrogenase.

We successfully carried out one-step conversion of methane to methanol using the 20Z_M2 strain without the addition of any chemical inhibitor of MDH and exogenous NADH. The 20Z_M2 was cultured on medium containing glycerol for 24 h, and methane was introduced to the headspace at a concentration of 50 % (v/v). As a result, methanol was accumulated to a concentration of 11.6 mM after 3 days with a yield of 0.484 g methanol g^{-1} methane (Fig. 7A, Table S2). The methanol production obtained here was higher than methanol production achieved from whole-cell *M. alcaliphilum* 20Z biocatalyst which showed the titre was only 0.022 mM (Patel et al., 2016).

Even though we successfully demonstrated that bioconversion of methane to methanol using microbial cell factory system without the addition of any chemical inhibitor of MDH and reducing power-generating sources such as formate, the yield of this
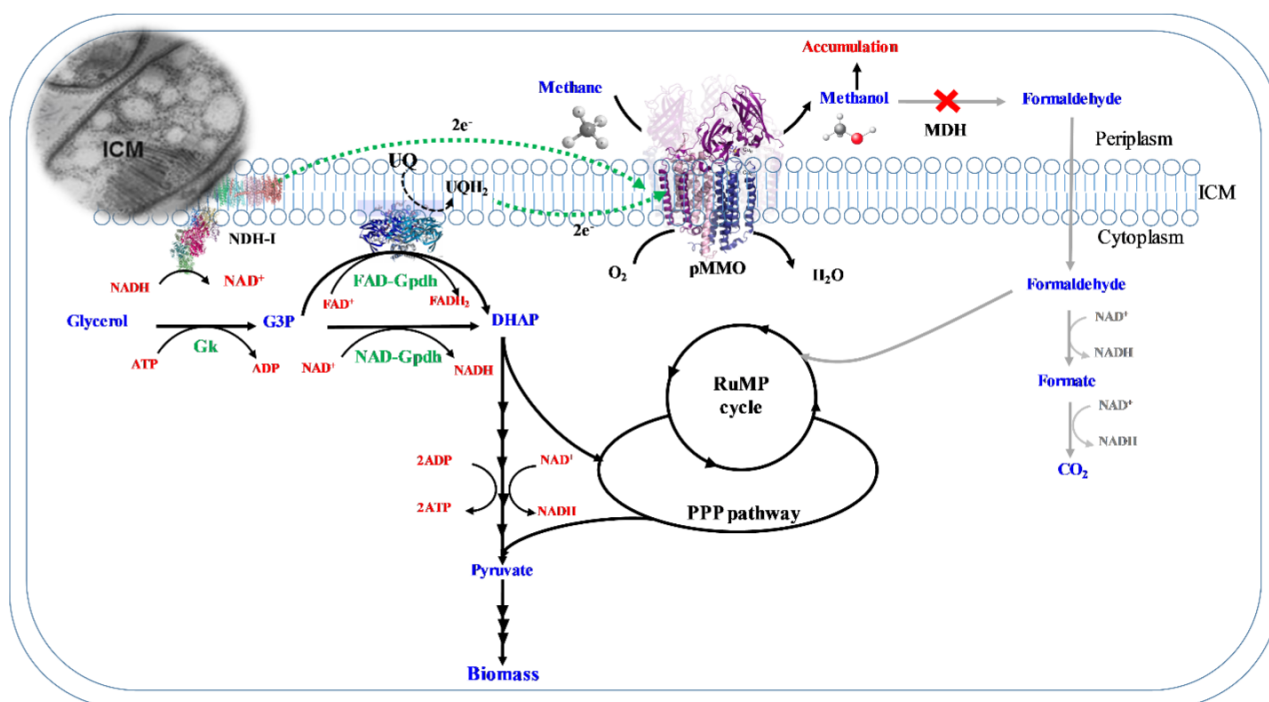
Fig. 6. One-step biological conversion of methane to methanol. To accumulate methanol without using inhibitors, *mxaF* and *xoxF* genes of a glycerol-utilizing strain of *M. alcaliphilum* 20Z were knocked out to prevent expression of methanol dehydrogenase. To support growth of the mutant strain, glycerol is used as a co-substrate with methane and plays a main role in cell growth, and methane is directly converted to methanol by pMMO. In addition, glycerol metabolism is proposed to provide reducing equivalents in terms of NADH and $FADH_2$, which deposit their electrons to quinone pool via other membrane components such as the complex I/NADH dehydrogenase (NDH-I) or FAD^+-dependent G3P dehydrogenase and are subsequently used to activate particulate methane monooxygenase (pMMO). UQ: Ubiquinone, UQH_2: Ubiquinol, ICM: intracytoplasmic membrane. Gk: glycerol kinase, FAD-Gpdh: FAD^+ dependent glycerol 3-phosphate dehydrogenase, NAD-Gpdh: NAD^+ dependent glycerol 3-phosphate dehydrogenase, Mdh: Methanol dehydrogenase, DHAP: dihydroxyacetone phosphate, G3P: glycerol 3-phosphate.
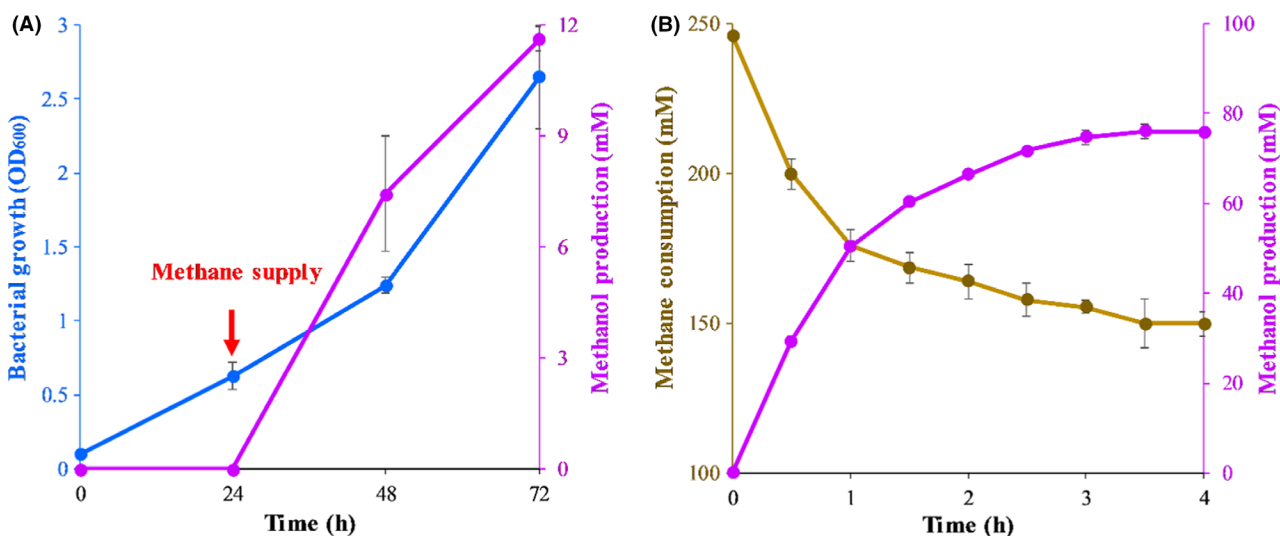

Fig. 7. (A) Conversion of methane to methanol using living cells of 20Z_M2 strain cultured in a shake flask. Cells were cultured on glycerol for 24 h; the headspace of the shake flask was refreshed with 50% (v/v) methane every 24 h for 72 h.
B. Conversion of methane to methanol using resting cells of 20Z_M2 strain. The reactions were carried out using 2.29 g DCW l^{-1} (OD600: 6.8) resting cell with 30% (v/v) methane in the presence of 40 mM formate, buffer pH 7. Data represent mean and standard derivation (SD) of two independent experimental replicates.

bioconversion was rather lower than expected. In general, it is difficult to gain theoretical yield due to several reasons. Firstly, it should be considered that methane-to-methanol conversion also requires NADH as a second substrate while reducing power generated from glycerol metabolism is not only used for methane conversion but also for making ATP via electron transport chain to maintain cell metabolism. Even though methane is captured into cell cytoplasm, but it does not mean that 100% percentage of methane is trapped by methane monooxygenase and converted into methanol due to deficiency of reducing power as well as the distribution of MMO units on intracytoplasmic membrane system in case of cell growth on glycerol. Therefore, supply of reducing equivalents-generating sources is useful to enhance activity of MMO (Hwang et al., 2015, Oh et al., 2019). Secondly, it might be due to methanol excretion rate constraint as well as non-specific oxidation of produced methanol by certain alcohol dehydrogenases which can convert methanol to downstream products, although the catalytic efficiency is low compared to methanol dehydrogenase. Therefore, reaction systems mimicking ideal conditions such as the cell-free system in the absence of other enzymes that degrade the product need to be developed to enhance the yield of products.

To overcome drawbacks from using living cells as a biocatalyst, we also designed a whole-cell biocatalyst to convert methane to methanol using non-growing resuspended cells or resting cells of 20Z_M2 strain. This approach could support facilitating product separation or preventing secondary reactions or undesired metabolites during cell growth, which could affect the bioconversion (Jackson et al., 2019). To do this, mutant cells were firstly cultured on glycerol to gain high optical density, and then, resting cells were used as a biocatalyst. Since glycerol is only used for cell growth phase not for biotransformation phase, this might cause the lack of NADH source for bioconversion of methane to methanol. To overcome this issue, 40 mM sodium formate was added to replenish NADH. Reaction process was carried out in 20 ml serum bottles with 30% (v/v) methane in the headspace. As a result, conversion yield was enhanced up to 79% with 76 mM methanol accumulated during 3.5 h (Fig. 7B). Obviously, the use of resting cells may be a good alternative to gain higher bioconversion yield which is limited by living cells. Therefore, the optimization of some factors such as additional reducing power source, increased optical density or downstream processing might help to further enhance bioconversion yield of methane to methanol using living cells for fermentative process.

In summary, we demonstrated a novel framework for direct conversion of methane to methanol in the absence of inhibitors and exogenous NADH. We expect this strategy to be applied for conversion of other alkanes that correspond to primary alcohols using methanotrophic biocatalyst.

Experimental procedures

Bacterial strains and growth conditions

The strains and plasmids used in this study are presented in Table 1. *Methylotuvimicrobium* (previously *Methylomicrobium*) *alcaliphilum* 20Z wild type and its engineered strains were cultured in 50 ml of nitrate mineral salts medium in a 500 mL baffled flask sealed with a screw cap at 30°C and 230 rpm. Methane was supplied to a final concentration of 50% (v/v) by gas substitution using a gas-tight syringe, and the headspace was refreshed daily. In addition, 1% (v/v) methanol also was used as carbon and energy sources for culture of *M. alcaliphilum* 20Z. Because crude glycerol contains methanol as an impurity (Yang et al., 2012, He et al., 2017), which is naturally utilized by *M. alcaliphilum* 20Z, we decided to use pure glycerol in this study to demonstrate this strain can efficiently utilize glycerol as a carbon and energy sources with a ranges of 0.1%, 0.5%, and 1% (v/v) for culture of engineered strains. The optical density of cell cultures was measured with a Beckman spectrophotometer using 1.5 ml cuvettes and a 1 cm path length. Kanamycin, gentamicin and zeocin were used to select both *M. alcaliphilum* 20Z and *Escherichia coli* strains containing recombinant plasmids, with a final concentration of 50 μg ml^{-1}, 10 μg ml^{-1} and 30 μg ml^{-1}, respectively.

Materials and tools for genetic modifications

All plasmids in this study were constructed using Gibson assembly. The primers and procedures used to construct expression vectors can be found in Table S1. These plasmids were transformed into *M. alcaliphilum* 20Z by electroporation as previously described (Nguyen et al., 2018). Genomic DNA of *E. coli* and *M. alcaliphilum* 20Z was isolated by a Wizard Genomic DNA Purification Kit (Promega, Madison, WI, USA). A Gibson assembly master mix was purchased from NEB (Hitchin, UK). Polymerase chain reaction (PCR) used Lamp Pfu polymerase (BioFACT, Daejeon, South Korea). A PCR purification kit and a gel extraction kit were supplied by Geneall (South Korea). Oligonucleotides and DNA sequencing were synthesized and performed by Macrogen (South Korea). Plasmid vector pAWP89 was linearized by inverse PCR using pAWP89-For/pAWP89-Rev. The genes *glpF*, *glpK*, *glpD*, *glpA* and *dhaK* were amplified via PCR using the genomic DNA of *E. coli* W3110, and *gpsA* was amplified using genomic DNA from *M. alcaliphilum* 20Z.

Table 1. Strains and plasmids used in this study.

Characteristic (s)	Relevant features	References
Strain		
E. coli DH5α	Cloning host	Invitrogen
M. alcaliphilum 20Z	Wild type, used as host strain	DMSZ
20Z_FKD	*M. alcaliphilum* 20Z harbouring pAWP89-FKD plasmid	This study
20Z_KD	*M. alcaliphilum* 20Z harbouring pAWP89-KD plasmid	This study
20Z_FKDA	*M. alcaliphilum* 20Z harbouring pAWP89-FKDA plasmid	This study
20Z_FAK	*M. alcaliphilum* 20Z harbouring pAWP89-FAK plasmid	This study
20Z_FKDA_*budABC*	20Z_FKDA with three-gene cluster *budABC* integration	This study
20Z_M2	20Z_FKDA with deletion of *mxaF* and *xoxF* genes	This study
Plasmid		
pAWP89	Expression vector, P_{tac}, Km^R	Puri et al. (2015)
pCM351	Deletion/integration vector, Gm^R	Marx and Lidstrom, (2002)
pAWP89_KD	pAWP89 derivative carrying the *glpK*, and *glpD* genes from *E. coli* str. K-12 substr. W3110	This study
pAWP89_FKD	pAWP89 derivative carrying the *glpK*, and *glpD* genes from *E. coli* str. K-12 substr. W3110	This study
pAWP89_FKDA	pAWP89 derivative carrying the *glpF*, *glpK* and *glpD* genes from *E. coli* str. K-12 substr. W3110, and *gpsA* from genome of *M. alcaliphilum* 20Z	This study
pAWP89_FAK	pAWP89 derivative carrying the *glpF*, *glpA*, and *dhaK* genes from *E. coli* W3110	This study
pBudK.p	pAWP89-based backbone carrying P_{tac} promoter and 2,3-BDO gene cluster originated from *Klebsiella pneumoniae* KCTC 224	Nguyen et al. (2018)
pCM351_*glgA1*	Variant of pCM351 GenT containing flanks of glycogen synthase encoded gene (*glgA1*)	Nguyen et al. (2018)
pCM351_*budABC*	pCM351_*glgA1* derivative carrying three-gene cluster *budABC* for integration	This study
pCM351_F1F2_*xoxF*	Variant of pCM351 GenT containing flanks to knock out *xoxF* gene	This study
pCM351_F1F2_*mxaF*	Variant of pCM351 GenT containing flanks to knock out *mxaF* gene	This study

These templates were then assembled with a linearized pAWP89 backbone. Chromosomal integration of the 2,3-BDO biosynthesis pathway was performed to replace glycogen synthase gene, *glgA1*. The 2,3-BDO gene cluster from *Klebsiella pneumoniae* under control of a P_{tac} promoter was amplified from pBudK.p (Nguyen et al., 2018), which subsequently was ligated into a pCM351-glgA1 vector that harboured two flank sequences of *glgA1* to generate pCM351-*budABC*. For methanol dehydrogenase removing, the gentamicin and zeocin resistance gene cassettes and the two regions flanking the *mxaF* and *xoxF* genes (600–800 base pairs) were assembled by Gibson assembly-based fusion PCR. The resulting products were purified and directly electroporated into the glycerol utilizing strain of *M. alcaliphilum* 20Z.

Gene expression analysis for 2.3 BDO production

Plasmid-based expression and genome-integrated expression of three genes *budA*, *budB* and *budC* were examined using real-time qPCR in *M. alcaliphilum* 20Z on methane. Total RNA samples were extracted following to previous protocol (Nguyen et al., 2020b) and directly used for RT-qPCR experiments. The primers used for RT-qPCR were provided in Table S1. A total RNA amount of 200 ng was firstly used for cDNA synthesis using a RevertAid First Strand cDNA Synthesis Kit (Thermo Scientific, Waltham, MA, USA) and subsequently used as a template for RT-qPCR. RT-qPCR was performed by using GoTaq qPCR Master Mix (Promega, Madison, WI, USA) in CFX Connect Real-Time PCR Detection System (Bio-Rad, Hercules, CA, USA). The cycle threshold (C_t) value for each gene was determined and normalized to the *rpoD* housekeeping gene (Miura et al., 2015, Bai et al., 2020). The relative expression between two samples was calculated by using the $\Delta\Delta C_t$ method (Henard et al., 2017).

Cytoplasmic NADH, NAD^+ extraction

The extraction protocol was modified from the previous work (He et al., 2016) as a conceptual basis. Bacterial cultures were collected at mid-log phase with the same density (approximately OD_{600} nm of 2.5–13 × 10^8 cells ml^{-1}). After centrifugation at 15 000 rpm for 5 min, the remaining pellets were resuspended in 400 μl 0.2 M NAOH and 0.2 M HCl for NADH and NAD^+ extraction, respectively. The cell lysates were incubated at 50°C for 15 min and immediately placed in ice water. Then, the cell lysates were neutralized by adding 400 μl 0.2 M HCl or 0.2 M NAOH, and subsequently were centrifuged at 15 000 rpm for 5 min. The supernatants were collected and stored at −20°C until analysis.

Analytical methods

The supernatant from the shake flask cultures was separated from cells by centrifugation. The supernatant was

then filtered through a 0.22-μm pore and stored at −20°C for high-performance liquid chromatography (HPLC). Quantities of 2,3-BDO, methanol and glycerol consumption were measured using HPLC (Jasco Co., Easton, PA, USA) with an Aminex HPX-87H organic acid column (Bio-Rad) and a refractive index detector. Sulphuric acid (0.005 M) was used as the mobile phase at 60 °C and a flow rate of 0.7 ml min^{-1}.

Cytoplasmic NADH, NAD$^+$ was quantified by HPLC with a LC column (250 × 4.6 mm; Phenomenex, Torrance, CA, USA) using UV detector at 260 nm. A 90:10 ratio of ammonium acetate (50 mM) and acetonitrile (100%) was used as the mobile phase at 35°C and a flow rate of 1 ml min^{-1}.

Methane consumption was quantified using a Younglin 6500GC gas chromatography equipped with a flame ionization detector (FID), and nitrogen was used as a carrier gas with a flow rate of 2.0 ml min^{-1}. In addition, a HP5-PlotQ capillary column was used with the oven temperature was maintained at 150°C. The injector and detector temperatures were set at 230 and 230°C, respectively.

Statistical analysis

Results are shown as mean ± SD (standard deviation). *T*-test statistical analysis was performed to calculate *P* values from the mean values of the indicated data. Asterisks were marked for significant difference (*$P < 0.05$).

Conflict of interest

The authors declare that they have no conflict of interest.

Author contributions

H.T.Q.L, A.D.N and Y.R.P carried out the experimental procedures, performed a complete analysis and prepared a draft of the manuscript. E.Y.L coordinated the study and finalized the manuscript. All authors read and approved the manuscript.

References

Akberdin, I.R., Thompson, M., Hamilton, R., Desai, N., Alexander, D., Henard, C.A., *et al.* (2018) Methane utilization in *Methylomicrobium alcaliphilum* 20Z R: a systems approach. *Sci Rep* **8:** 2512.

Applebee, M.K., Joyce, A.R., Conrad, T.M., Pettigrew, D.W., and Palsson, B.Ø. (2011) Functional and metabolic effects of adaptive glycerol kinase (GLPK) mutants in *Escherichia coli*. *J Biol Chem* **286:** 23150–23159.

Bai, B., Ren, J., Bai, F., and Hao, L. (2020) Selection and validation of reference genes for gene expression studies in *Pseudomonas brassicacearum* GS20 using real-time quantitative reverse transcription PCR. *PLOS One* **15:** e0227927.

Bennett, R.K., Steinberg, L.M., Chen, W., and Papoutsakis, E.T. (2018) Engineering the bioconversion of methane and methanol to fuels and chemicals in native and synthetic methylotrophs. *Curr Opin Biotech* **50:** 81–93.

Booth, I.R. (2005) Glycerol and methylglyoxal metabolism. In *Escherichia coli and Salmonella: Cellular and Molecular Biology*. Neidhardt, F.C., Curtiss, R., Ingraham, J.L., Lin, E.C.C., Low, K.B., *et al.* (eds). Washington, DC, USA: ASM Press, **1.**

Bordel, S., Rodríguez, Y., Hakobyan, A., Rodríguez, E., Lebrero, R., and Muñoz, R. (2019) Genome scale metabolic modeling reveals the metabolic potential of three Type II methanotrophs of the genus Methylocystis. *Metab Eng* **54:** 191–199.

Clomburg, J.M., Crumbley, A.M., and Gonzalez, R. (2017) Industrial biomanufacturing: the future of chemical production. *Science* **355:** aag0804.

do Carmo Dias, B., Lima, M.E.d.N.V., Vollú, R.E., da Mota, F.F., da Silva, A.J.R., de Castro, A.M. et al. (2018) 2, 3-Butanediol production by the non-pathogenic bacterium *Paenibacillus brasilensis*. *Appl Microbiol Biotechnol* **102:** 8773–8782.

Durnin, G., Clomburg, J., Yeates, Z., Alvarez, P.J., Zygourakis, K., Campbell, P., and Gonzalez, R. (2009) Understanding and harnessing the microaerobic metabolism of glycerol in *Escherichia coli*. *Biotechnol Bioeng* **103:** 148–161.

Gonzalez, R., Murarka, A., Dharmadi, Y., and Yazdani, S.S. (2008) A new model for the anaerobic fermentation of glycerol in enteric bacteria: trunk and auxiliary pathways in *Escherichia coli*. *Metab Eng* **10:** 234–245.

Haynes, C.A., and Gonzalez, R. (2014) Rethinking biological activation of methane and conversion to liquid fuels. *Nat Chem Biol* **10:** 331.

He, A.-Y., Yin, C.-Y., Xu, H., Kong, X.-P., Xue, J.-W., Zhu, J., *et al.* (2016) Enhanced butanol production in a microbial electrolysis cell by *Clostridium beijerinckii* IB4. *Bioproc Biosys Eng* **39:** 245–254.

He, Q., McNutt, J., and Yang, J. (2017) Utilization of the residual glycerol from biodiesel production for renewable energy generation. *Renew Sustain Energy Rev* **71:** 63–76.

Henard, C.A., Smith, H.K., and Guarnieri, M.T. (2017) Phosphoketolase overexpression increases biomass and lipid yield from methane in an obligate methanotrophic biocatalyst. *Metab Eng* **41:** 152–158.

Hwang, I.Y., Hur, D.H., Lee, J.H., Park, C.-H., Chang, I.S., Lee, J.W., and Lee, E.Y. (2015) Batch conversion of methane to methanol using *Methylosinus trichosporium* OB3b as biocatalyst. *J Microbiol Biotechnol* **25:** 375–380.

Hwang, I.Y., Lee, S.H., Choi, Y.S., Park, S.J., Na, J.G., Chang, I.S., *et al.* (2014) Biocatalytic conversion of methane to methanol as a key step for development of methane-based biorefineries. *J Microbiol Biotechnol* **24:** 1597–1605.

Hwang, I.Y., Nguyen, A.D., Nguyen, T.T., Nguyen, L.T., Lee, O. K., and Lee, E.Y. (2018) Biological conversion of methane to chemicals and fuels: technical challenges and issues. *Appl Microbiol Biotechnol* **102:** 3071–3080.

Jackson, E., Ripoll, M., and Betancor, L. (2019) Efficient glycerol transformation by resting Gluconobacter cells. *MicrobiologyOpen* **8:** e926.

Kalyuzhnaya, M.G., Puri, A.W., and Lidstrom, M.E. (2015) Metabolic engineering in methanotrophic bacteria. *Metab Eng* **29:** 142–152.

Kamachi, T., and Okura, I. (2018) Methanol Biosynthesis Using Methanotrophs. In *Methane biocatalysis: Paving the way to sustainability*. Kalyuzhnaya, M. G., and Xing, X.-H. (eds). Cham: Springer International Publishing, pp. 169–182.

Kang, T.S., Korber, D.R., and Tanaka, T. (2014) Metabolic engineering of a glycerol-oxidative pathway in *Lactobacillus panis* PM1 for utilization of bioethanol thin stillage: potential to produce platform chemicals from glycerol. *Appl Environ Microbiol* **80:** 7631–7639.

Kanno, M., and Atsumi, S. (2017) Engineering an obligate photoautotrophic cyanobacterium to utilize glycerol for growth and chemical production. *ACS Synthetic Biol* **6:** 69–75.

Keller, P., Noor, E., Meyer, F., Reiter, M.A., Anastassov, S., Kiefer, P., and Vorholt, J.A. (2020) Methanol-dependent *Escherichia coli* strains with a complete ribulose monophosphate cycle. *Nat Commun* **11:** 5403.

Kim, H.J., Huh, J., Kwon, Y.W., Park, D., Yu, Y., Jang, Y.E., *et al.* (2019) Biological conversion of methane to methanol through genetic reassembly of native catalytic domains. *Nat Catalysis* **2:** 342–353.

Li, Z., Yan, J., Sun, J., Xu, P., Ma, C., and Gao, C. (2018) Production of value-added chemicals from glycerol using in vitro enzymatic cascades. *Commun Chem* **1:** 71.

Marx, C.J., and Lidstrom, M.E. (2002) Broad-host-range cre-lox system for antibiotic marker recycling in gram-negative bacteria. *BioTechniques* **33:** 1062–1067.

Maurel, C., Reizer, J., Schroeder, J.I., Chrispeels, M.J., and Saier, M.H. Jr (1994) Functional characterization of the *Escherichia coli* glycerol facilitator, GlpF, in Xenopus oocytes. *J Biol Chem* **269:** 11869–11872.

Miura, C., Komatsu, K., Maejima, K., Nijo, T., Kitazawa, Y., Tomomitsu, T., *et al.* (2015) Functional characterization of the principal sigma factor RpoD of phytoplasmas via an in vitro transcription assay. *Sci Rep* **5:** 11893.

Miyaji, A., Nitta, M., and Baba, T. (2019) Influence of copper ions removal from membrane-bound form of particulate methane monooxygenase from *Methylosinus trichosporium* OB3b on its activity for methane hydroxylation. *J Biotechnol* **1:** 100001.

Mustakhimov, I.I., But, S.Y., Reshetnikov, A.S., Khmelenina, V.N., and Trotsenko, Y.A. (2016) Homo- and heterologous reporter proteins for evaluation of promoter activity in *Methylomicrobium alcaliphilum* 20Z. *Appl Biochem Microbiol* **52:** 263–268.

Nguyen, A.D., Hwang, I.Y., Lee, O.K., Kim, D., Kalyuzhnaya, M.G., Mariyana, R., et al. (2018) Systematic metabolic engineering of *Methylomicrobium alcaliphilum* 20Z for 2, 3-butanediol production from methane. *Metab Eng* **47:** 323–333.

Nguyen, A.D., Kim, D., and Lee, E.Y. (2020a) Unlocking the biosynthesis of sesquiterpenoids from methane via the methylerythritol phosphate pathway in methanotrophic bacteria, using α-humulene as a model compound. *Metab Eng* **61:** 69–78.

Nguyen, A.D., Nam, G., Kim, D., and Lee, E.Y. (2020b) Metabolic role of pyrophosphate-linked phosphofructokinase pfk for C1 assimilation in *Methylotuvimicrobium alcaliphilum* 20Z. *Microb Cell Fact* **19:** 131.

Nomanbhay, S., Hussein, R., and Ong, M.Y. (2018) Sustainability of biodiesel production in Malaysia by production of bio-oil from crude glycerol using microwave pyrolysis: a review. *Green Chem Lett Rev* **11:** 135–157.

Oh, S., Hwang, I., Lee, O., Won, W., and Lee, E. (2019) Development and optimization of the biological conversion of ethane to ethanol using whole-cell methanotrophs possessing methane monooxygenase. *Molecules* **24:** 591.

Patel, S.K., Jeong, J.H., Mehariya, S., Otari, S.V., Madan, B., Haw, J.R., *et al.* (2016) Production of methanol from methane by encapsulated *Methylosinus sporium*. *J Microbiol Biotechnol* **26:** 2098–2105.

Peyraud, R., Schneider, K., Kiefer, P., Massou, S., Vorholt, J.A., and Portais, J.-C. (2011) Genome-scale reconstruction and system level investigation of the metabolic network of *Methylobacterium extorquens* AM1. *BMC Syst Biol* **5:** 189.

Puri, A.W., Owen, S., Chu, F., Chavkin, T., Beck, D.A., Kalyuzhnaya, M.G., and Lidstrom, M.E. (2015) Genetic tools for the industrially promising methanotroph *Methylomicrobium buryatense*. *Appl Environ Microbiol* **81:** 1775–1781.

Rho, H.S., and Choi, K. (2018) Cofactor regeneration using permeabilized *Escherichia coli* expressing NAD (P)+-dependent glycerol-3-phosphate dehydrogenase. *J Microbiol Biotechn* **28:** 1346–1351.

Rittmann, D., Lindner, S.N., and Wendisch, V.F. (2008) Engineering of a glycerol utilization pathway for amino acid production by *Corynebacterium glutamicum*. *Appl Environ Microbiol* **74:** 6216–6222.

Rugbjerg, P., Myling-Petersen, N., Porse, A., Sarup-Lytzen, K., and Sommer, M.O.A. (2018) Diverse genetic error modes constrain large-scale bio-based production. *Nat Commun* **9:** 787.

Rugbjerg, P., and Sommer, M.O.A. (2019) Overcoming genetic heterogeneity in industrial fermentations. *Nat Biotechnol* **37:** 869–876.

Sirajuddin, S., Barupala, D., Helling, S., Marcus, K., Stemmler, T.L., and Rosenzweig, A.C. (2014) Effects of zinc on

particulate methane monooxygenase activity and structure. *J Biol Chem* **289**: 21782–21794.

Strong, P., Kalyuzhnaya, M., Silverman, J., and Clarke, W. (2016) A methanotroph-based biorefinery: potential scenarios for generating multiple products from a single fermentation. *Bioresour Technol* **215**: 314–323.

Szymanowska-Powałowska, D. (2015) The effect of high concentrations of glycerol on the growth, metabolism and adaptation capacity of *Clostridium butyricum* DSP1. *Electron J Biotechnol* **18**: 128–133.

Uppada, V., Bhaduri, S., and Noronha, S.B. (2014) Cofactor regeneration–an important aspect of biocatalysis. *Curr Sci* 946–957.

Voegele, R., Sweet, G., and Boos, W. (1993) Glycerol kinase of *Escherichia coli* is activated by interaction with the glycerol facilitator. *J Bacteriol* **175**: 1087–1094.

Vuilleumier, S., Khmelenina, V.N., Bringel, F., Reshetnikov, A.S., Lajus, A., Mangenot, S., *et al.* (2012) Genome sequence of the haloalkaliphilic methanotrophic bacterium *Methylomicrobium alcaliphilum* 20Z. *Am Soc Microbiol* **194**: 551–552.

Weckbecker, A., Gröger, H., and Hummel, W. (2010) Regeneration of nicotinamide coenzymes: principles and applications for the synthesis of chiral compounds. In: *Biosystems Engineering I*. Berlin: Springer, pp. 195-242.

Weissenborn, D.L., Wittekindt, N., and Larson, T.J. (1992) Structure and regulation of the GlpFK operon encoding glycerol diffusion facilitator and glycerol kinase of *Escherichia coli* K-12. *J Biol Chem* **267**: 6122–6131.

West, C.A., Salmond, G.P., Dalton, H., and Murrell, J.C. (1992) Functional expression in *Escherichia coli* of proteins B and C from soluble methane monooxygenase of *Methylococcus capsulatus* (Bath). *J Gen Microbiol* **138**: 1301–1307.

Woolston, B.M., King, J.R., Reiter, M., Van Hove, B., and Stephanopoulos, G. (2018) Improving formaldehyde consumption drives methanol assimilation in engineered *E. coli*. *Nat Commun* **9**: 2387.

Yang, F., Hanna, M.A., and Sun, R. (2012) Value-added uses for crude glycerol–a byproduct of biodiesel production. *Biotechnol Biofuels* **5**: 13.

Yang, Z., and Zhang, Z. (2018) Production of (2R, 3R)-2, 3-butanediol using engineered *Pichia pastoris*: strain construction, characterization and fermentation. *Biotechnol Biofuels* **11**: 35.

Zhan, Y., Sheng, B., Wang, H., Shi, J., Cai, D., Yi, L., *et al.* (2018) Rewiring glycerol metabolism for enhanced production of poly-γ-glutamic acid in *Bacillus licheniformis*. *Biotechnol Biofuels* **11**: 306.

Zhang, L., Tang, Y., Guo, Z., and Shi, G. (2013) Engineering of the glycerol decomposition pathway and cofactor regulation in an industrial yeast improves ethanol production. *J Ind Microbiol Biot* **40**: 1153–1160.

Zhang, Z., Kuipers, G., Niemiec, Ł., Baumgarten, T., Slotboom, D.J., de Gier, J.-W., and Hjelm, A. (2015) High-level production of membrane proteins in *E. coli* BL21(DE3) by omitting the inducer IPTG. *Microb Cell Fact* **14**: 142.

Supporting information

Additional supporting information may be found online in the Supporting Information section at the end of the article.

Fig. S1. Growth rate of glycerol-utilizing strain 20Z_FKD and wild-type *M. alcaliphilum* 20Z on 0.1% (v/v) glycerol.

Fig. S2. Growth rate of 20Z_M2 on 0.1% (v/v) glycerol and 1% (v/v) methanol as the carbon sources.

Fig. S3. Confirmation of unmarked deletions of *mxaF* and *xoxF* of 20Z_M2 via PCR (M-marker, WT-wild-type, 1-4: unmarked deletion of *mxaF*, 5-8: unmarked deletion of *xoxF*).

Table S1. Primers used in this study.

Table S2. The titers of methanol by *M. alcaliphilum* 20Z from previous studies.